Title: Anti-inflammatory effects and molecular mechanisms of 8-prenyl quercetin

Authors: Ayami Hisanaga[a], Rie Mukai[b], Kozue Sakao[a, c], Junji Terao[b], De-Xing Hou [a, c, ¶]

Affiliations: [a]United Graduate School of Agricultural Science, Kagoshima University, Kagoshima, Japan. [b]Department of Food Science, Institute of Health Biosciences, University of Tokushima Graduate School, Tokushima, Japan. [c]Faculty of Agriculture, Kagoshima University, Kagoshima, Japan.

[¶]Corresponding author: Professor De-Xing Hou, Faculty of Agriculture, Kagoshima University, Korimoto 1-21-24, Kagoshima, 890-0065, Japan.

E-mail: hou@chem.agri.kagoshima-u.ac.jp (D.-X Hou), Fax/Tel: +81 99 285 8649

Abbreviations:

COX-2, cyclooxygenase-2; ERK, extracellular signal-regulated kinase; FBS, fetal bovine serum; FITC, fluorescein isothiocyanate; G-CSF, granulocyte colony-stimulating factor; GM-CSF, granulocyte-macrophage colony-stimulating factor; IFN-γ, interferon-gamma; IL-1α (3, 6, 9, 13, 17), interleukin-1 alpha (3, 6, 9, 13, 17); iNOS, inducible nitric oxide synthase; *i.p.*, intraperitoneally; JNK, Jun-*N*-terminal kinase; LPS, lipopolysaccharide; MAPK, mitogen-activated protein kinase; MCP-1, monocyte chemotactic protein-1; MEK, MAPK/ERK kinase; NO, nitric oxide; NF-κB, nuclear factor-kappa B; PGE_2 , prostaglandin E_2; PQ, 8-prenyl quercetin; Q, quercetin; SAPK, stress-activated protein kinase; SEK, SAPK/Erk kinase (MKK4); *s.c.*, subcutaneously; TLR4, Toll-like receptor 4; TNF-α, tumor necrosis factor alpha.

Scope: 8-prenyl quercetin (PQ) is a typical prenylflavonoid distributed in plant foods and shows higher potential bioactivity than its parent quercetin (Q) although the mechanisms are not fully understood. This study aims to clarify the anti-inflammatory effects and molecular mechanisms of PQ in cell and animal models, compared to Q. **Methods and results:** RAW264.7 cells were treated with PQ or Q to investigate the influence on the production of inducible nitric oxide synthase (iNOS), cyclooxygenase-2 (COX-2) and protein kinases by Western blotting. Nitric oxide (NO) and prostaglandin E_2 (PGE_2) were measured by the Griess method and ELISA, respectively. Cytokines were assayed by the multiplex technology. Mouse paw edema was induced by lipopolysaccharide (LPS). The results revealed that PQ had stronger inhibition on the productions of iNOS, COX-2, NO, PGE_2, and 12 kinds of cytokines, than Q. PQ also showed *in vivo* anti-inflammatory effect by attenuating mouse paw edema. Molecular data revealed that PQ had no competitive binding to Toll-like receptor 4 (TLR4) with LPS, but directly targeted SEK1-JNK1/2 and MEK1-ERK1/2. **Conclusion:** PQ as a potential inhibitor revealed anti-inflammatory effect in both cell and animal models at least by targeting SEK1-JNK1/2 and MEK1-ERK1/2.

Keywords: Prenyl quercetin / Inflammatory mediators / Cellular signaling / Direct binding / Molecular targets

1 Introduction

Prenylflavonoids are naturally occurring flavonoids possessing a C5 isoprenoid unit in a diphenylpropane structure. The roots, leaves and seeds of *Moraceace, Leguminosae* and *Asteraceae* are major sources of prenylflavonoids although more than 1000

prenylflavonoids have been found in the plants [1, 2]. In recent years, their potential benefits for human health have been considered because prenylflavonoids are reported to have antibacterial, antioxidant and estrogenic activities [3]. It is noticed that prenylation of flavonoids could enhance their biological functions and bioavailability. For example, prenylation of naringenin and genistein enhanced their estrogenicity [4]. Prenylated naringenin also enhanced the accumulation of naringenin in muscle tissue, resulting in the prevention of muscle atrophy in rodent model [5]. Thus, molecular mechanisms of prenylflavonoids should be taken into account to estimate the biological functions.

Quercetin (Q) is a representative compound of naturally occurring flavonoid present in many vegetables and fruits [6]. Extensive data have indicated that Q has many biological functions [7, 8, 9]. Recent studies have demonstrated that Q has anti-inflammatory effects in both mouse macrophage cell [10] and rat models [11]. Moreover, 8-prenyl quercetin (PQ) is found in *Desmodium caudatum* [12] that is a traditional herb used for anti-inflammation in Japan [13]. Thus, we challenge to clarify the effect and molecular mechanisms of anti-inflammation by PQ, compared to its parent Q.

During inflammatory disease, the primary cells of chronic inflammation are macrophages that produce excess amounts of mediators such as nitric oxide (NO), prostaglandin E_2 (PGE_2), and pro-inflammatory cytokines [14], which play pivotal roles in consequences of inflammation [15]. Although the cellular signaling pathways regulating the inflammation are very complicated, mitogen-activated protein kinase (MAPK) and nuclear factor-kappa B (NF-κB) pathways have been suggested to be key pathways for the regulations of inflammatory mediator expressions [14]. MAPK can stimulate the production of inflammatory mediators such as inducible nitric oxide

77 synthase (iNOS), cyclooxygenase-2 (COX-2) and cytokines in bacterial
78 lipopolysaccharide (LPS)-activated macrophages [16, 17, 18]. Moreover, recent several
79 lines of studies have showed that polyphenolic compounds could directly bind to
80 MAPK proteins to attenuate the kinase signaling. For example, myricetin [19],
81 procyanidin B2 [20] could directly bind to MAPK/ERK kinase (MEK) to suppress
82 MEK phosphorylation and downstream signaling.
83 Based on the properties of prenylflavonoids and the information of inflammation
84 processes, we investigated the anti-inflammatory effects and molecular mechanisms of
85 PQ, compared to Q. First of all, we used mouse macrophage-like cells (RAW264.7),
86 which can be stimulated with LPS to mimic a status of infection and inflammation, to
87 screen the influence of PQ on the productions of iNOS, NO, COX-2, PGE_2, and
88 cytokines. Then, we confirmed the *in vivo* anti-inflammatory effects of PQ using a
89 mouse paw edema model. Finally, we investigated the modulation of PQ on
90 LPS-induced inflammatory signaling pathway, and challenged to clarify the molecular
91 targets of PQ by chemical biology approaches.
92

93 # 2 Materials and methods

94 ## 2.1 Materials

95 PQ (Fig. 1A) was synthesized as described previously [21]. Q (Fig. 1B) was purchased
96 from Sigma (St. Louis, MO, USA). PQ and Q were dissolved in DMSO (0.2% final
97 concentration in cultural medium). LPS and fluorescein isothiocyanate (FITC)
98 conjugated-LPS (*Escherichia coli* Serotype 055:B5) were from Sigma (St. Louis, MO,
99 USA). The antibodies against iNOS, COX-2, MEK1, α-tubulin and anti-goat IgG-HRP
100 were from Santa Cruz Biotechnology Inc. (Santa Cruz, CA, USA). The other antibodies
101 were from Cell Signaling Technology (Beverly, MA, USA). CNBr-activated Sepharose

4B was from GE Healthcare.

2.2 Cell culture

RAW264.7 cells were purchased from the American Type Culture Collection (Manassas, VA, USA) and cultured in Dulbecco's modified Eagle's medium containing 10% fetal bovine serum (FBS), 4 mM *L*-glutamine, and 2 mM Penicillin-Streptomycin Mixed Solution. After pre-culture for 24 h, the cells were starved in serum-free medium to eliminate the influence of FBS. The cells were then treated for 30 min with PQ or Q or DMSO as control vehicle (0.2% final concentration of DMSO in cultural medium) before exposure to 40 ng/mL LPS for the indicated times in each experiment.

2.3 Measurement of nitrite and PGE_2

Nitrite was measured to estimate NO production with the Griess method [22]. In brief, RAW264.7 macrophage cells (1×10^6 cells/dish) were seeded into 6-cm dish. The cells culture and treatments were described in Section 2.2, and the culture medium from each dish was collected after LPS treatment for 12 h. The nitrite concentration in the culture medium was detected by the reaction with the Griess reagent for 10 min at room temperature, and the absorbance was measured at 550 nm wavelength.

PGE_2 in cultural medium was measured with a PGE_2 enzyme immunoassay kit (Cayman Co., St. Louis, MO) according to manufacturer's manual [23]. In brief, RAW264.7 cells (1.2×10^5 cells/well) were seeded into each well of 12-well plates. The cells culture and treatments were described in Section 2.2, and the culture medium from each well was collected after LPS treatment for 12 h. The level of PGE_2 released into culture medium was determined by measuring absorbance at 405 nm in a microplate reader.

2.4 Cytokine determination by the multiplex technology

The method has been described in our previous report [24]. In brief, RAW264.7 cells (1.2×10^5 cells/well) were seeded into each well of 12-well plate. The cells culture and treatments were described in Section 2.2, and the culture medium from each well was collected after LPS treatment for 12 h. The levels of cytokines in culture medium was measured with Bio-Plex Pro Mouse Cytokine 23-Plex Panel kit (Bio-Rad Laboratories) including IL-1α, IL-1β, IL-2, IL-3, IL-4, IL-5, IL-6, IL-9, IL-10, IL-12(p40), IL-12(p70), IL-13, IL-17, Eotaxin, G-CSF, GM-CSF, IFN-γ, KC, MCP-1, MIP-1α, MIP-1β, RANTES and TNF-α. The assay was performed with a Bio-Plex machine (Bio-Plex 200 System, Bio-Rad) according to the manufacturer's instructions, and the data were analyzed with the Bio-Plex manager software (version 5.0).

2.5 Western blotting

Western blotting was performed as described previously [22]. In brief, RAW264.7 cells (1×10^6 cells/dish) were seeded into each 6-cm dish. The cell culture and treatments were described in Section 2.2. The cells were lysed in a lysis buffer, and boiled for 5 min. Approximately 20-60 μg of proteins were run on 10% SDS-PAGE and then transferred to PVDF membrane (GE Healthcare, UK). The blotted membrane was incubated with specific primary antibody overnight at 4 °C and further incubated for 1 h with HRP-conjugated secondary antibody. Bound antibodies were detected by ECL agent and further quantified by Lumi Vision Imager software (TAITEC Co., Japan).

2.6 *In vivo* paw edema model

The animal experiments were conducted in accordance with the guidelines of the

Animal Care and Use Committee of Kagoshima University (Permission N0. A12005). Male ICR mice (4 weeks old) from Japan SLC Inc were group-housed under controlled light (12 h light/day) and temperature (25 °C). All the animals had free access to water and feed in a home cage. The mice were randomly divided into four groups: control, LPS, LPS plus PQ or Q. PQ or Q was dissolved in PBS containing 2% DMSO and administered to the mice in 1 μM/kg for PQ or 2 μM/kg for Q by intraperitoneal (*i.p.*) injection for 4 days. LPS were then injected subcutaneously (*s.c.*) to paw in a dose of 1 mg/kg. Paw thickness was measured using caliper (model 19975, Shinwa Rules Co. Ltd) before and every hour after LPS treatment until 3 h. After 3 h, mice were sacrificed and blood serums were collected from heart. The serums without any dilution were used to detect IL-6 by mouse ELISA Ready-SET-Go kit (eBioscience) according to manufacturer's instructions.

2.7 Flow cytometric assay

The competition assay of PQ and LPS for Toll-like receptor 4 (TLR4) was performed by flow cytometry using the FITC-conjugated LPS [25]. RAW264.7 cells (5×10^5 cells/ml in serum-free medium) were treated with or without PQ (15 μM) or cold-LPS (non FITC-conjugated LPS) (100 ng/ml) for 30 min before expose to FITC-LPS (10 ng/ml) for 30 min. After washing, the fluorescence emitted was analyzed at FL1 (530 nm) with flow cytometer (CyFlow, Partec).

2.8 Molecular modeling

Computer modeling was performed as described previously [26]. The modeling of PQ or Q to TLR4 (PDB ID: 3FXI) [27, 28], SEK1 (PDB ID: 2DYL) [29], JNK1 (PDB ID: 3PZE), MEK1 (PDB ID: 1S9J) [29], and ERK2 (PDB ID: 2Y9Q) was performed using

177 Molecular Operating Environment TM software (MOE, Version 2012.10, Chemical
178 Computing Group Inc.). Hydrogen atoms were first added, and force field (MMFF94x)
179 atomic charges were assigned. Docking of PQ or Q to protein was done using
180 MOE-ASEDock 2013 software [30].
181
182 **2.9 *Ex vivo* pull-down assay**
183 *Ex vivo* pull-down assay was performed as described in our previous paper [26].
184 Briefly, PQ and Q (5 μM) were coupled to CNBr-activated Sepharose 4B beads (25 mg)
185 in a coupling buffer [0.5 M NaCl, 0.1 M $NaHCO_3$ (pH 8.3) and 25 % DMSO] for
186 overnight at 4 °C according to the manufacturer's instructions. The mixture was washed
187 with 5 volumes of coupling buffer and then resuspended by 5 volumes of 0.1 M
188 Tris-HCl buffer (pH 8.0) for 2 h rotation at room temperature (RT) to block any
189 remaining active groups. After washing three cycles with acetate buffer [0.1 M acetic
190 acid (pH 4.0) and 0.5 M NaCl], the conjugated beads were further washed by wash
191 buffer [0.1 M Tris-HCl (pH 8.0) and 0.5 M NaCl]. The RAW264.7 cell lysates (500
192 μg/ml) were then incubated overnight at 4 °C with Sepharose 4B beads, PQ- or
193 Q-conjugated Sepharose 4B beads (100 μl, 50% slurry) in a reaction buffer [50 mM
194 Tris-HCl (pH 8.5), 5 mM EDTA, 150 mM NaCl, 1mM DTT, 0.01% Nonidet P-40, 2
195 μg/ml BSA, 0.02 mM PMSF and 1 μg protease inhibitor cocktail]. The beads were
196 washed 5 times with 50 mM Tris-HCl (pH 7.5) containing 5 mM EDTA, 200 mM NaCl,
197 1 mM DTT, 0.02% Nonidet P-40 and 0.02 mM PMSF. The proteins bound to the beads
198 were detected by Western blotting with each specific antibody.
199
200 **2.10 Statistical analysis**
201 The difference between treated and control cells were analyzed by analysis of variance

tests or Tukey's test. A probability of $p < 0.05$ was considered significant.

3 Results

3.1 The inhibitory effects of PQ and Q on the production of inflammatory factors

To investigate the effect of PQ and Q on the production of inflammatory factors, we first used LPS-activated RAW264.7 cells [14]. As shown in Fig. 2A and 2B, the productions of LPS-induced iNOS and COX-2 protein were significantly suppressed by PQ and Q in dose-dependent manner. PQ almost completely suppressed the productions at 15 μM while Q slightly did even at 30 μM. PQ had two-fold stronger inhibition than Q. Since iNOS and COX-2 are the enzymes to synthesize NO and PGE_2, respectively, we next examined the effects of PQ and Q on the productions of NO and PGE_2 in such treatment. A parallel inhibitory effects by PQ and Q were observed in LPS-induced nitrite (Fig. 2C and 2D) and PGE_2 (Fig. 2E and 2F) production. These results indicated that the effective dose for the inhibition is 15 μM for PQ or 30 μM for Q, thus, we used 15 μM PQ and 30 μM Q for the following cell experiments.

We further examined the levels of 23 kinds of cytokines in the culture medium of treated cells as described in Section2. LPS treatment for 12 h enhanced more than five-fold level of G-CSF, TNF-α, RANTES, IL-6, MCP-1, GM-CSF, more than two-fold level of IL-12 (p70), KC, MIP-1β, IL-1α, IL-10, IL-9; and less than two-fold in IL-13, IL-1β, IL-4, IL-17, IL-3, IFN-γ, IL-12 (p40), Eotaxin, IL-5, MIP-1α, IL-2, compared to that of the cells without LPS treatment [24]. Pretreatment with PQ or Q at the indicated concentrations decreased significantly the level of IL-1α, IL-6, IFN-γ, TNF-α, IL-3, IL-9, IL-13, GM-CSF, Eotaxin, IL-17, G-CSF, and MCP-1 (Fig. 3), but did not affect significantly other 11 kinds of cytokines (data not shown). PQ also had stronger inhibition for these pro-inflammatory cytokines than Q.

3.2 Inhibition of LPS-induced paw edema in mice

To confirm the anti-inflammatory effects of PQ and Q *in vivo,* we used the model of mouse paw edema induced by LPS (Fig. 4A) as described previously [24]. The results showed that LPS treatment increased significantly the paw thickness with maximum after 1 h and following down after 2 h. Pretreatment with 1 μM/kg PQ or 2 μM/kg Q for 4 days reduced significantly LPS-induced paw thickness during this period, compared with LPS treatment alone. As controls, treatment with PBS or PQ or Q only in 2 % DMSO did not show any effect on paw edema (Fig. 4B). Simultaneously, we checked the serum level of pro-inflammatory IL-6 by ELISA. As shown in Fig. 4C, pretreatment with 1 μM/kg PQ or 2 μM/kg Q decreased significantly the level of LPS-induced IL-6. These data confirmed the anti-inflammatory effect of PQ or Q *in vivo*.

3.3 The effect of PQ and Q on the binding of LPS to TLR4.

TLR4 is a specific receptor for LPS to initiate the inflammatory responses. Our data showed that the productions of LPS-induced inflammatory mediators were suppressed by PQ and Q in both cell and mouse models. We wonder whether PQ or Q binds to TLR4 competitively with LPS to block LPS-induced inflammation. Therefore, we first performed computational analysis based on the structure of TLR4-MD2 complex (PDB ID: 3FXI) and PQ or Q. As shown in Fig. 5A, both PQ and Q docked in the most same region of TLR4-MD2 complex with three hydrogen bonds for PQ, and with four hydrogen bonds for Q. The PQ or Q binding region is different with LPS binding region, suggesting that PQ and Q may have no competition binding to TLR4-MD2 complex with LPS. To confirm this, we further used FITC-conjugated LPS to investigate whether PQ or Q binds to TLR4 competitively with LPS by flow cytometric assay (see Section

2). As shown left panel in Fig. 5B, treatment with FITC-conjugated LPS produced a strongest peak of fluorescence that could be suppressed by adding 10-fold of cold-LPS, suggesting the FITC-conjugated LPS worked in this cell system. Next, we added PQ or Q in this assay system. As shown right panel in Fig. 5B, PQ addition did not reduce the fluorescent strength. These data further support that PQ and Q may have no competitive binding to TLR4-MD2 complex with LPS although PQ or Q itself shows fluorescence in this wavelength. Thus, these data suggest that PQ or Q might exert anti-inflammatory action by targeting cytoplasmic protein kinases.

3.4 Modulation of PQ and Q on MAPK signaling

Our data revealed that the inhibition of PQ or Q on inflammatory factors is not due to its competitive binding to TLR4. It is recently noticed that PQ or Q can efflux the cells [31, 32] and modulate MAPK signaling to regulate pro-inflammatory mediators. Thus, we investigated the effects of PQ and Q on the LPS-induced phosphorylation of MAPK in RAW264.7 cells. The cells were treated with 15 μM PQ or 30 μM Q for 30 min before exposure to 40 ng/ml LPS for 30 min. As shown in Fig. 6, PQ suppressed markedly phosphorylation of SEK1-JNK1/2 and MEK1-ERK1/2 signaling while Q only slightly suppressed them. Both PQ and Q did not suppress the phosphorylation of MKK3/6-p38 (data not shown).

3.5 Binding ability of PQ and Q to SEK1-JNK1/2 and MEK1-ERK1/2

Our data suggest that SEK1-JNK1/2 and MEK1-ERK1/2 are potential targets for PQ and Q to inhibit inflammatory signaling. Thus, we investigated whether the PQ and Q bind to each protein kinase directly, using bead-bound pulldown assay which has been validated as effective screening tool in our previous study [26]. PQ or Q is coupled with

CNBr-sepharose 4B beads, and then incubated with protein lysate extracted from RAW264.7 cells. Bound protein kinase was detected by Western blotting with antibody after washing out. As shown in Fig. 7A, SEK1 and JNK1/2 were detected in the Sepharose 4B beads coupled with PQ (54.2% and 31.6% binding rate) and with Q (31.6% and 12.6% binding rate), but was not detected in the Sepharose 4B beads alone. As the same fashion, MEK1 and ERK1/2 were detected in the Sepharose 4B beads coupled with PQ (75.6% and 77.3% binding rate), and with Q (21.2% and 37.1 % binding rate), but was not detected in the Sepharose 4B beads alone (As shown in Fig. 7B). These data showed that PQ and Q could bind directly to SEK1, JNK1/2, MEK1 and ERK1/2. Moreover, PQ had stronger binding activity to these protein kinases than Q.

3.6 Docking model between PQ/Q and SEK1-MEK1 kinases

To know how PQ or Q binds to SEK1 and MEK1 kinases, we performed computer modeling of PQ or Q bound to these protein kinases, using the software as described in Section 2. The results provided the interesting information that three hydrogen bonds were formed between PQ and Glu175 and Asp259 residues of MKK4 (SEK1), which configured nearby ATP-binding pocket in left panel, and four hydrogen bonds were formed between Q and Glu175, Asp259, and Asp277 residues of MKK4 (SEK1), which configured a part of ATP-binding pocket in right panel. The domains for PQ and Q binding are very close, almost the same. As shown in Fig. 8B, two hydrogen bonds were formed between PQ and Lys55 and Asp151 residues of JNK1, which configured a part of ATP-binding pocket in right panel, and three hydrogen bonds were formed between Q and Val80, Glu109, and Lys166 residues of JNK1, which configured a part of ATP-binding pocket in left panel. The domains for PQ and Q binding are in different

302 domains. Three hydrogen bonds were formed between PQ and Arg181, Glu182 and
303 Asp351 residues of MEK1 (Fig.8C), which configured a part of MEK1 catalytic domain
304 in right panel. Two hydrogen bonds were formed between Q and Asp365 of MEK1,
305 which configured a part of MEK1 catalytic domain in left panel. The domains of MEK1
306 for PQ and Q binding are different (Fig.8C). Four hydrogen bonds were formed
307 between PQ and Asp251, Lys272 and Asp291 residues of ERK2 (Fig. 8D), which
308 configured a part of ERK2 catalytic domain in left panel, and four hydrogen bonds were
309 formed between Q and MEK1, same as PQ in left panel. These docking results support
310 our pull-down binding data between PQ or Q and SEK1-MEK1 kinases.
311

312 **4 Discussion**

313 In the present study, we investigated the anti-inflammatory effects and molecular
314 mechanisms of 8-prenyl quercetin, compared to its parent quercetin, in both cell and
315 animal models. In the cell model, we demonstrated that PQ had more than two-fold
316 stronger inhibition on LPS-induced productions of pro-inflammatory factors (iNOS, NO,
317 COX-2, PGE_2) and cytokines (IL-1α, IL-6, IFN-γ, TNF-α, IL-3, IL-9, IL-13, GM-CSF,
318 Eotaxin, IL-17, G-CSF, and MCP-1, IL-12 (p70), TNF-α, and MCP-1). In the animal
319 model, we observed that PQ also showed more than two-fold stronger inhibition on
320 mouse paw edema (Fig. 4). Thus, our data suggested that PQ is more potential inhibitor
321 for LPS-induced inflammation than its parent form.
322 The issues concerned are the molecular mechanisms that how PQ suppressed
323 LPS-induced inflammation. TLR4 is an important sensor for LPS by enhancing the
324 binding of LPS to MD-2 to form LPS-TLR4-MD2 complex to trigger signaling
325 cascades that involve activation of MAPK, NF-κB, and anti-inflammatory mediators

326 [33]. We wonder whether PQ and Q compete with LPS for binding to TLR4. To clarify
327 this, we first performed computational docking analysis based on the structure of
328 TLR4-MD2 complex (PDB ID: 3FXI) and PQ or Q. The data showed that both PQ and
329 Q docked in the different domain of TLR4-MD2 complex with LPS, suggesting that PQ
330 and Q might have no competitive binding to TLR4-MD2 complex with LPS. To confirm
331 this, we further used FITC-conjugated LPS to investigate whether PQ or Q has
332 competitive binding with TLR4 by flow cytometric assay. Our data showed that both
333 PQ and Q did not reduce the fluorescent strength by FITC-conjugated LPS, further
334 supporting that PQ and Q might have no competitive binding to TLR4-MD2 complex
335 with LPS. These data suggest that PQ and Q might attenuate cellular inflammatory
336 signaling by inhibiting the activation of cellular protein kinases.
337 MAPK signaling is one of the important cell signaling pathways that regulate
338 cytokines and pro-inflammatory mediators such as IL-1, IL-6, TNF-α, and iNOS during
339 inflammatory response although the cellular signaling pathways regulating
340 inflammation are very complicated. We first investigated the potential of PQ and Q
341 binding to MAP kinases by the bead-bound pulldown assay, which has been validated
342 as an effective screening tool in our previous study [26]. SEK1-JNK1/2 and
343 MEK1-ERK1/2 were detected in the Sepharose 4B beads coupled with PQ and cellular
344 lysate, but not found in Sepharose 4B beads alone (Fig. 7). These data supported that
345 PQ might target the signaling molecules of SEK1-JNK1/2 and MEK1-ERK1/2 by direct
346 binding. Furthermore, we performed computer modeling of PQ and Q bound to
347 SEK1-JNK1/2 and MEK1-ERK1/2, using the software of three dimensional
348 pharmacophore modeling for the interaction of a small molecule with protein. The
349 results provided the interesting information that several hydrogen bonds were found
350 between the hydroxyl groups of PQ or Q and amino acid residues of SEK1-JNK1/2 and

MEK1-ERK1/2 (Fig. 8A- 8D).

Moreover, the docking domain by PQ or Q is not completely located in the ATP-binding pocket of these protein kinases, but configured nearby or a part of ATP-binding pocket. These data at least suggest that PQ or Q may dock these domains to modulate the 3D-structure of these protein kinases to influence the phosphorylation, rather than competing with ATP. Our data indicate that the downregulation of SEK1-JNK1/2 and MEK1-ERK1/2 pathways by PQ or Q is at least involved in the inhibition of LPS-induced inflammation.

On the other hand, direct binding efficiency for PQ is 2-3 fold higher than that for Q although the binding domains of these protein kinases for PQ and Q were very close, almost the same. The reason may be related to the efficiency of cellular uptake and bioaccumulation. It is reported that prenylation increased the hydrophobicity and affinity of Q to hydrophobic phospholipid bilayer membranes [31], which might enhance the cellular uptake of flavonoids and result in their biological activities in *in vitro* model systems [3]. *In vivo* data confirmed that prenylation enhances accumulation of naringenin in mouse muscle tissue after long-term feeding, and accumulation of quercetin in liver tissue [5]. Therefore, our data could support that the higher direct binding efficiency for PQ may be due to its efficiency in cellular uptake and bioaccumulation enhanced by prenylation.

In summary, we demonstrated that 8-prenyl quercetin has stronger anti-inflammatory activity than its parent form *in vitro* and *in vivo*. Moreover, the downregulation of MAPK signaling pathways is at least involved in the inhibition of inflammatory mediators by PQ. Direct binding assay and molecule docking analysis revealed that SEK1-JNK1/2 and MEK1-ERK1/2 might be direct molecule targets for PQ. These results from cell and mouse models provide a comprehensive data for understanding the

anti-inflammatory effects and molecular mechanisms of PQ.

Acknowledgments

This work was partly supported by the fund of Scholar Research of Kagoshima University, and by the Program for Promotion of Basic and Applied Researches for Innovations in Bio-oriented Industry in Japan.

5 References

[1] Yazaki, K., Sasaki, K., Tsurumaru, Y., Prenylation of aromatic compounds, a key diversification of plant secondary metabolites. *Phytochemistry*, 2009, *70*, 1739-1745.

[2] Barron, D., Ibrahim, R. K., Isoprenylated flavonoids-A survey, *Phytochemistry*, 1996, *43*, 921-982.

[3] Chen, X., Mukwaya, E., Wong, M. S., et al., A systematic review on biological activities of prenylated flavonoids. *Pharm. Biol.* 2014, *52*, 655-660

[4] Kretzschmar, G., Zierau, O., Wober, J., et al., Prenylation has a compound specific effect on the estrogenicity of naringenin and genistein. *J. Steroid Biochem. Mol. Biol.* 2010, *118*, 1-6

[5] Mukai, R., Horikawa, H., Fujikura, Y., et al., Prevention of disuse muscle atrophy by dietary ingestion of 8-prenylnaringenin in denervated mice. *PLoS ONE*. 2012, *7*, e45048.

[6] Peterson, J., Dwyer, J., Flavonoids: Dietary occurrence and biochemical activity. *Nutr. Res.* 1998, *18*, 1995-2018.

[7] Moskaug, J.O., Carlsen, H., Myhrstad, M., et al., Molecular imaging of the biological effects of quercetin and quercetin-rich foods. *Mech. Ageing Dev.* 2004,

401 *125*, 315-324.
402 [8] Tanigawa, S., Fujii, M., Hou, D. X., Stabilization of p53 is involved in
403 quercetin-induced cell cycle arrest and apoptosis in HepG2 cells. *Biocsci.*
404 *Biotechnol. Biochem.* 2008, *72*, 797-804.
405 [9] Formica, J. V. and Regelson, W., Review of biology of querctin and related
406 bioflavonoids. *Fd Chem. Toxic.* 1995, *33*, 1061-1080.
407 [10] Cho, S. Y., Park, S. J., Kwon, M. J., et al., Quercetin suppresses proinflammatory
408 cytokines production through MAP kinases and NF-κB pathway in
409 lipopolysaccharide-stimulated macrophage. *Mol. Cell. Biochem.* 2003, *243*,
410 153-160.
411 [11] Comalada, M., Camesco, D., Sierra, S., et al., In vivo quercetin anti-inflammatory
412 effect involves release of quercetin, which inhibits inflammation through
413 down-regulation of the NF-κB pathway. *Eur. J. Immunol.* 2005, *35*, 584-592.
414 [12] Wu, Y., Luo, Q., Sun, C., et al., [Chemical constituents contained in Desmodium
415 caudatum]. *Zhongguo Zhong Yao Za Zhi.* 2012, *37*, 1788-1792.
416 [13] Sasaki, H., Kashiwada, Y., Shibatav, H., et al., Prenylated flavonoids from the roots
417 of Desmodium caudatum and evaluation of their antifungal activity. *Planta Med.*
418 2012, *78*, 1851-1856.
419 [14] Laskin, D. L., Laskin, J. D., Role of macrophages and inflammatory mediators in
420 chemically induced toxicity, *Toxicology*, 2001, *160*, 111-118.
421 [15] Hadad, J. J., Cytokines and related receptor-mediated signaling pathways,
422 *Biochem. Biophys. Res. Commun.* 2002, *297*, 700-713.
423 [16] Lu, Y. C., Yeh, W. C., Ohashi, P. S., LPS/TLR4 signal transduction pathway,
424 *Cytokine*, 2008, *42*, 145-151.
425 [17] Chang, L., Karin, M., Mammalian MAP kinase signalling cascades, *Nature,* 2001,

426 *410*, 37-40.
427 [18] Rossol, M., Heine, H., Meusch, U., et al., LPS-induced cytokine production in
428 human monocytes and macrophages. *Crit. Rev. Immunol.* 2011, *31*, 379-446.
429 [19] Lee, K. W., Kang, N. J., Rogozin, E. A., et al., Myricetin is a novel natural
430 inhibitor of neoplastic cell transformation and MEK1, *Carcinogenesis,* 2007, *28*,
431 1918-1927.
432 [20] Kang, N. J., Lee, K. W., Lee, D. E., et al., Cocoa procyanidins suppress
433 transformation by inhibiting mitogen-activated protein kinase kinase, *J. Biol. Chem.*
434 2008, *283*, 20664-20673.
435 [21] Kawamura, T., Hayashi, M., Mukai, R., et al., An efficient method for
436 c8-prenylation of flavonols and flavanones. *Synthesis.* 2012, *44*, 1308-1314.
437 [22] Uto, T., Fujii, M., Hou, D.-X., 6-(Methylsulfinyl)hexyl isothiocyanate suppresses
438 inducible nitric oxide synthase expression through the inhibition of Janus kinase
439 2-mediated JNK pathway in lipopolysaccharide-activated murine macrophages,
440 *Biochem. Pharmacol.* 2005, *70*, 1211-1221.
441 [23] Uto, T., Fujii, M., Hou, D.-X., Inhibition of lipopolysaccharideinduced
442 cyclooxygenase-2 transcription by 6-(methylsulfinyl) hexyl isothiocyanate, a
443 chemopreventive compound from *Wasabia japonica (Miq.)* Matsumura, in mouse
444 macrophages. *Biochem. Pharmacol.* 2005, *70*, 1772-1784.
445 [24] You, S., Nakanishi, E., Kuwata, H., et al., Inhibitory effects and molecular
446 mechanisms of garlic organosulfur compounds on the production of inflammatory
447 mediators. *Mol. Nutr. Food Res.* 2013, *57*, 2049-2060.
448 [25] Kim, J. K. and Jun, J. G. Ailanthoidol suppresses lipopolysaccharide-stimulated
449 inflammatory reactions in RAW264.7 cells and endotoxin shock in mice. *J. Cell.*
450 *Biochem.* 2011, *112*, 3816-3823.

[26] Kumamoto, T., Fujii, M., Hou, D. -X., Akt is a direct target for myricetin to inhibit cell transformation. *Mol. Cell Biochem.* 2009, *332*, 33-41.

[27] Xing, J., Li, R., Li, N., et al., Anti-inflammatory effect of procyanidin B1 on LPS-treated THP1 cells via interaction with the TLR4–MD-2 heterodimer and p38 MAPK and NF-κB signaling. *Mol. Cell Biochem.* 2015, *407*, 89-95.

[28] Park, B. S., Song, D. H., Kim, H, M., et al., The structural basis of lipopolysaccharide recognition by the TLR4-MD-2 complex. *Nature*, 2009, *458*, 1191-1196.

[29] Kim, J. E., Kwon, J. Y., Seo, S. K., et al, Cyanidin suppresses ultraviolet B-induced COX-2 expression in epidermal cells by targeting MKK4, MEK1, and Raf-1. *Biochem. Pharmacol*. 2010, *79*, 1473-1482.

[30] Goto , J., Kataoka, R., Muta, H., et al., ASEDock docking based on alpha spheres and excluded volumes. *J. Chem. Inf. Model.* 2008, *48*, 583-590.

[31] Mukai, R., Fujikura, Y., Murota, K., et al., Prenylation enhances quercetin uptake and reduces efflux in Caco-2 cells and enhances tissue accumulation in mice fed long-term. *J. Nutr.* 2013, *143*, 1558-1564.

[32] Tammela, P., Laitinen, L., Galkin, A., et al., Permeability characteristics and membrane affinity of flavonoids and alkyl gallates in Caco-2 cells and in phospholipid vesicles. *Arch. Biochem. Biophys.* 2004, *425*, 193-199.

[33] Akira, S., Takeda, K., and Kaisho, T., Toll-like receptors: critical proteins linking innate and acquired immunity. *Nat. Immunol.* 2001, *2*, 675-680.

476 **Figure Legends:**

477

478 **Figure 1.** The chemical structures of 8-prenyl quercetin (PQ) and quercetin (Q)

479

480 **Figure 2.** Influence of PQ and Q on the inflammatory mediators. PQ (A) and Q (B)
481 inhibited LPS-induced expression of iNOS and COX-2. RAW264.7 cells were treated
482 with the indicated concentrations of each sample for 30 min, and then exposed to 40
483 ng/ml LPS for 12 h. COX-2 and iNOS were detected by Western blotting as described
484 in Section 2. PQ (C, E) and Q (D, F) also inhibited the productions of LPS-induced NO
485 and PGE_2. RAW264.7 cells were treated as the same as above. The amount of nitrite (C,
486 D) and PGE_2 (E, F) in culture medium were measured as described in Section 2. Each
487 value represents the mean ±S.D. of triplicate cultures. Means with differently lettered
488 superscripts differ significantly each other at the probability of $p < 0.05$.

489

490 **Figure 3.** Influence of PQ and Q on the productions of LPS-induced cytokines. The
491 culture and treatment of RAW264.7 cells were performed as described in Figure 2. The
492 amounts of cytokines in culture medium were measured by the multi-plex technology as
493 described in Section 2. Each value represents the mean ± S.D. of triplicate cultures.
494 Means with asterisk superscripts differ significantly at the probability of $p < 0.05$.

495

496 **Figure 4.** Inhibition of PQ and Q on LPS-induced mouse paw edema. The mice were
497 divided into four groups: control, LPS, LPS plus PQ or Q, PQ or Q only. Each group
498 had three mice, respectively. PQ (1 μM/kg) or Q (2 μM/kg) was injected *i.p.* for 4 days,
499 and LPS (1 mg/kg) was then injected *s.c.* at mouse paw. The paw thickness was
500 measured using digital caliper before and every hour after LPS treatment until 3 h (A).

501 The change in paw edema thickness was shown in (B). Means with differently lettered
502 superscripts differ significantly against control at the probability of $p < 0.05$. The
503 change in level of serum IL-6 is shown in (C). The blood serums were obtained from
504 the mice that were treated with or without LPS for 3 h by collection of heart blood. The
505 serum IL-6 was measured as described in Section 2. Each value represents the mean ±
506 S.D. of three mice. Means with asterisk superscripts differ significantly at the
507 probability of $p < 0.05$.
508
509 **Figure 5.** (A) The models of PQ and Q docking to TLR4. Hydrogen bonds are indicated
510 by green lines in lower figure. *Blue ribbon*: TLR4 (Chain A), *green ribbon*: MD2
511 (Chain B), *orange*: PQ, *yellow*: Q, *red*: LPS (Color figure online). (B) The competitive
512 binding assay for PQ to TLR4 with FITC-conjugated LPS. RAW264.7 cells (5×10^5
513 cells/ml in serum-free medium) were treated with or without PQ (15 μM) or cold-LPS
514 (unlabeled-LPS) (100 ng/ml) for 30 min before exposure to FITC-LPS (10 ng/ml) for 30
515 min. After washing, the fluorescence emitted was analyzed with flow cytometry as
516 described in Section 2.
517
518 **Figure 6.** Suppression of PQ and Q on the phosphorylation of SEK1, JNK1/2, MEK1
519 and ERK1/2. RAW264.7 cells were pretreated with the indicated concentrations of PQ
520 or Q for 30 min, and then exposed to 40 ng/ml LPS for 30 min. The phosphorylated
521 protein kinases and α-tubulin were detected with their antibodies, respectively. The
522 induction fold of the phosphorylated kinase was calculated as the intensity of the
523 treatment relative to that of control normalized to α-tubulin by densitometry. The blots
524 shown are the examples of three separate experiments.
525

526 **Figure 7.** Binding abilities of PQ and Q to SEK1 and JNK1/2 (A), MEK1 and ERK1/2
527 (B). Whole cell lysate (input control, *lane 1*), lysate precipitation with Sepharose 4B
528 beads (negative control, *lane 2*), Sepharose 4B-PQ-coupled beads (*lane 3*), and
529 Sepharose 4B-Q-coupled beads (*lane 4*) were applied to SDS-PAGE and then detected
530 with SEK1, JNK1/2, MEK1 or ERK1/2 antibody, respectively. The binding efficiency
531 of each protein kinase to PQ or Q was presented as the ratio of input control,
532 respectively.
533
534 **Figure 8.** The models of PQ and Q docking to MKK4 (SEK1) (A), JNK1 (B), MEK1
535 (C), and ERK2 (D). Electrostatic potential surface is indicated in close-up figure of
536 upper side, and hydrogen bonds are indicated by blue and green lines in lower figure.
537 *Blue ribbon*: protein kinase, *red ribbon*: ATP-binding site, *orange*: PQ, *yellow*: Q (Color
538 figure online).

A

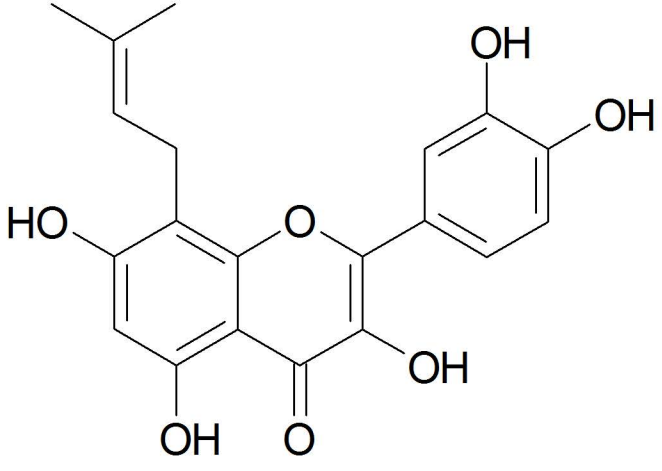

8-prenyl quercetin (PQ)

B

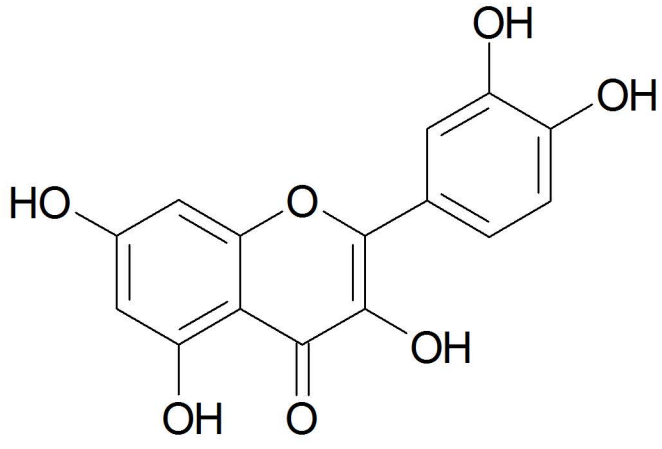

Quercetin (Q)

Fig.1 Hisanaga et al.

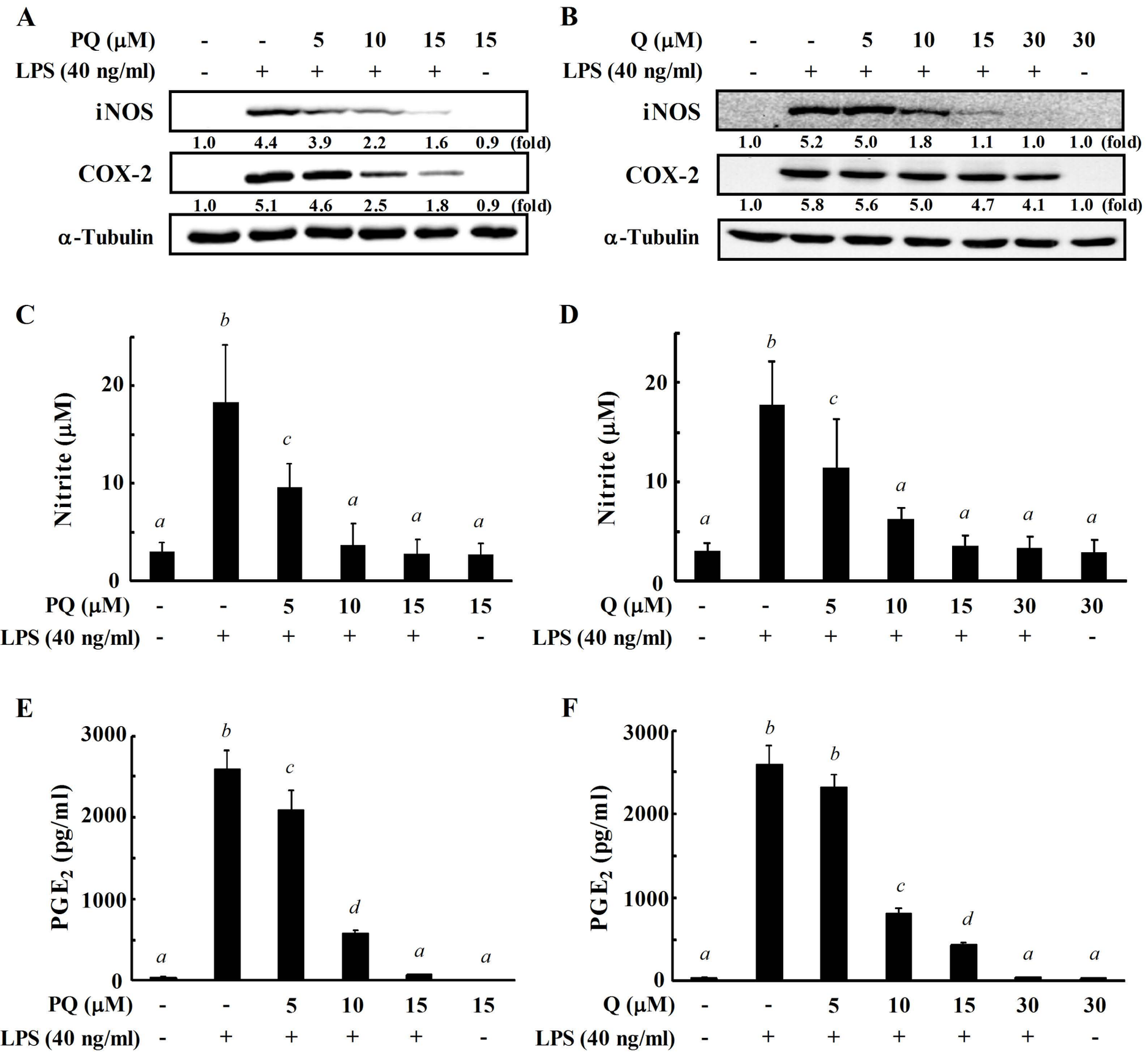

Fig.2 Hisanaga et al.

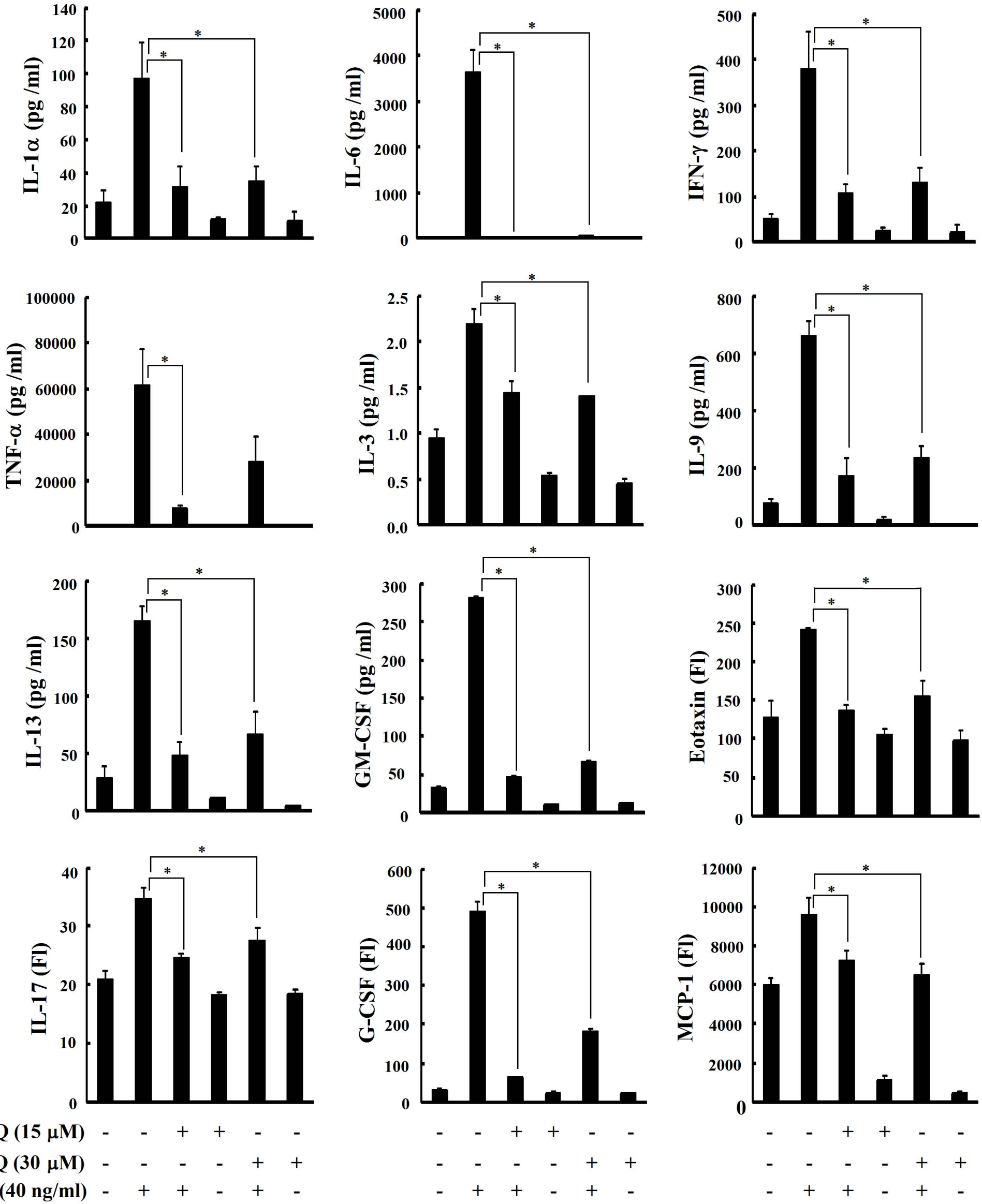

Fig.3 Hisanaga et al.

A

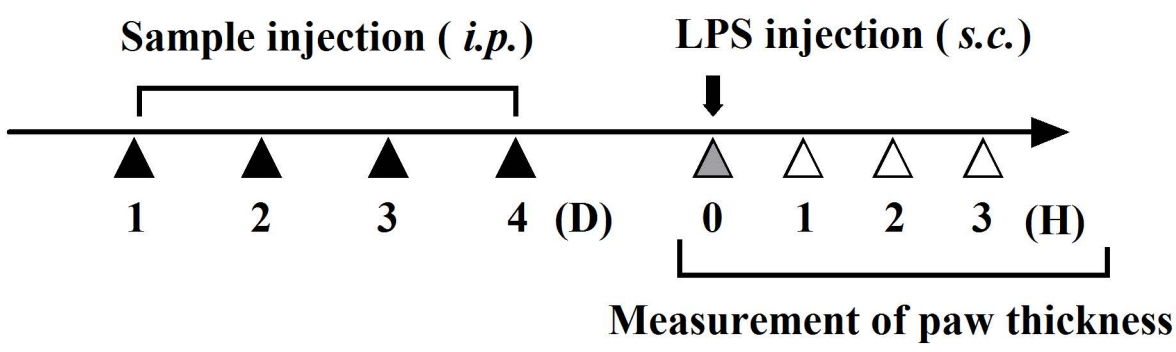

B

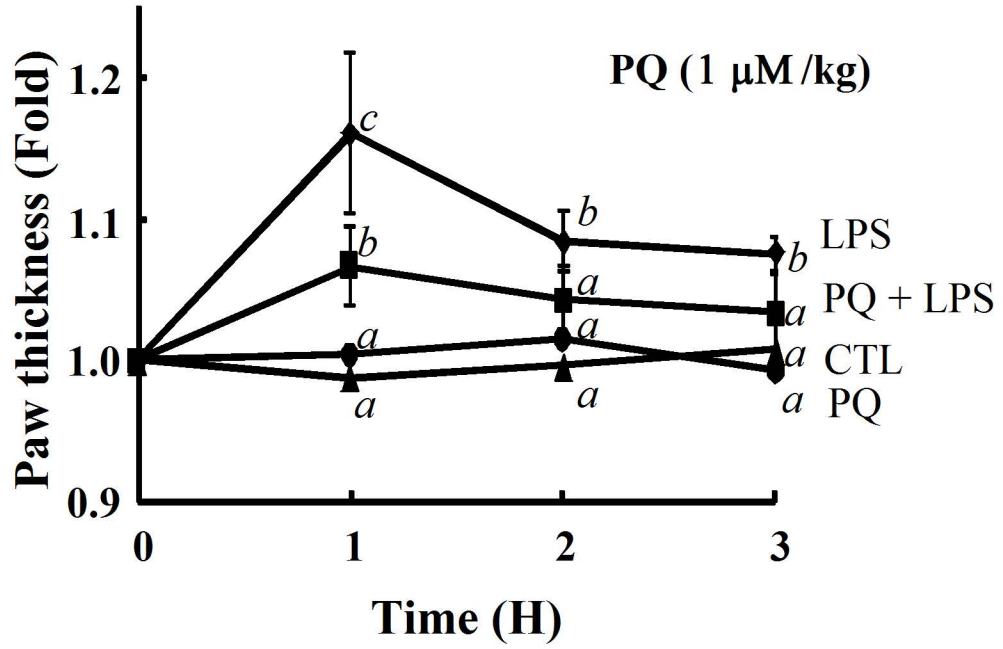

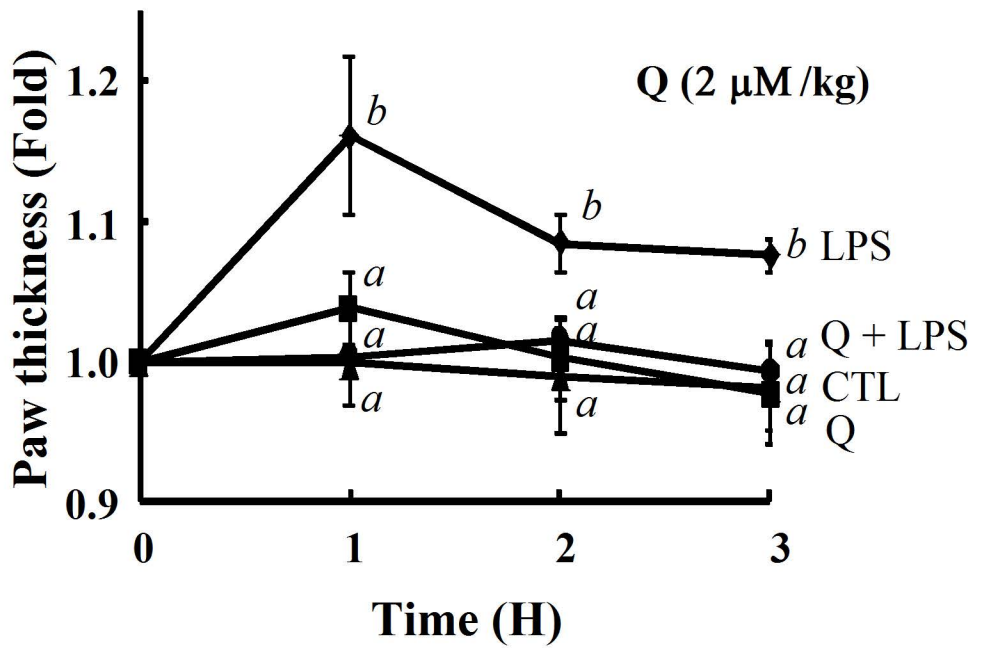

C

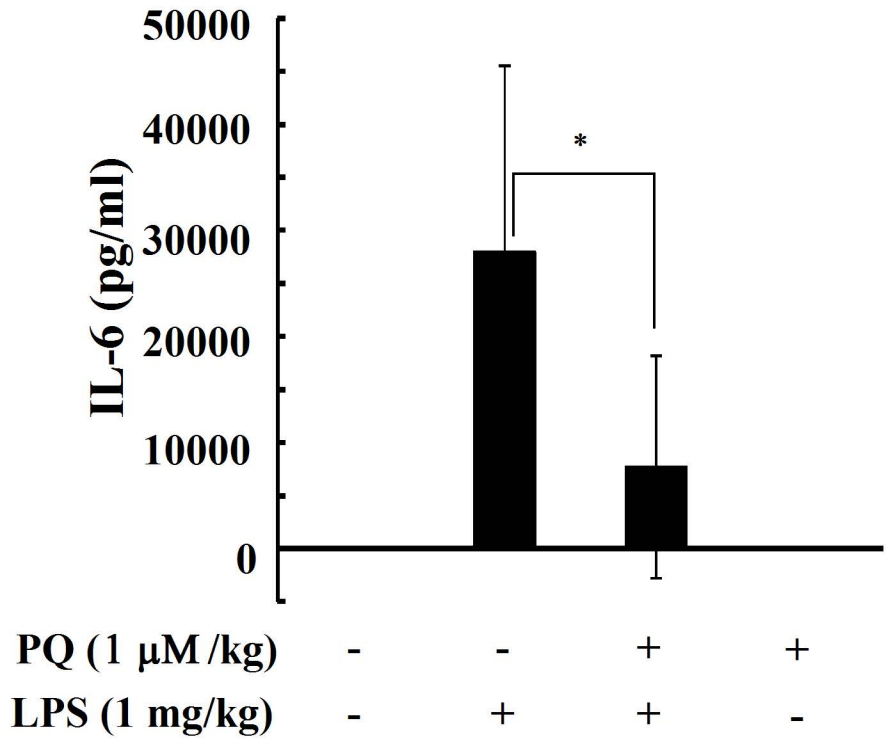

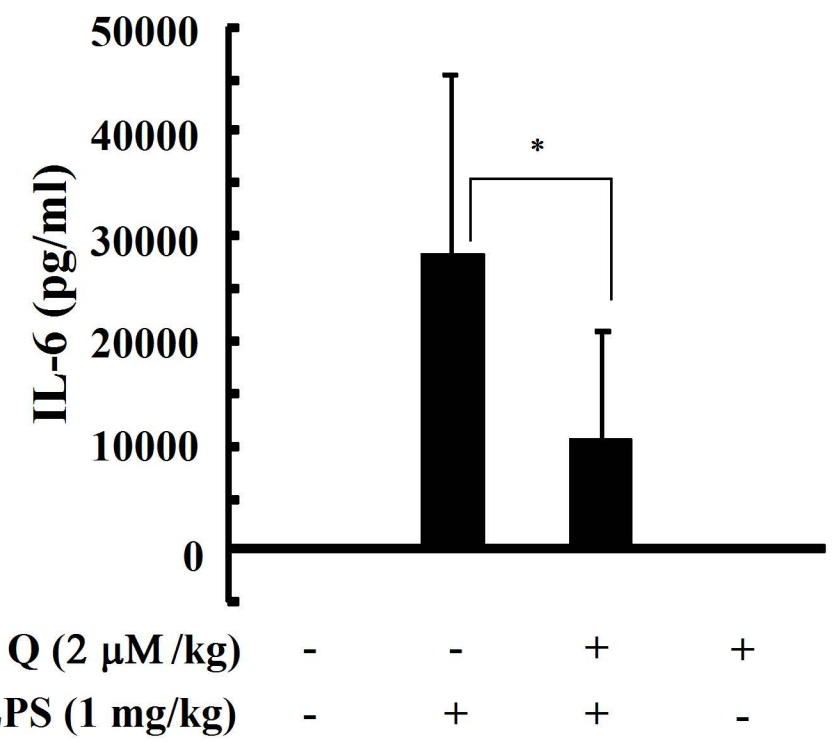

Fig.4 Hisanaga et al.

A

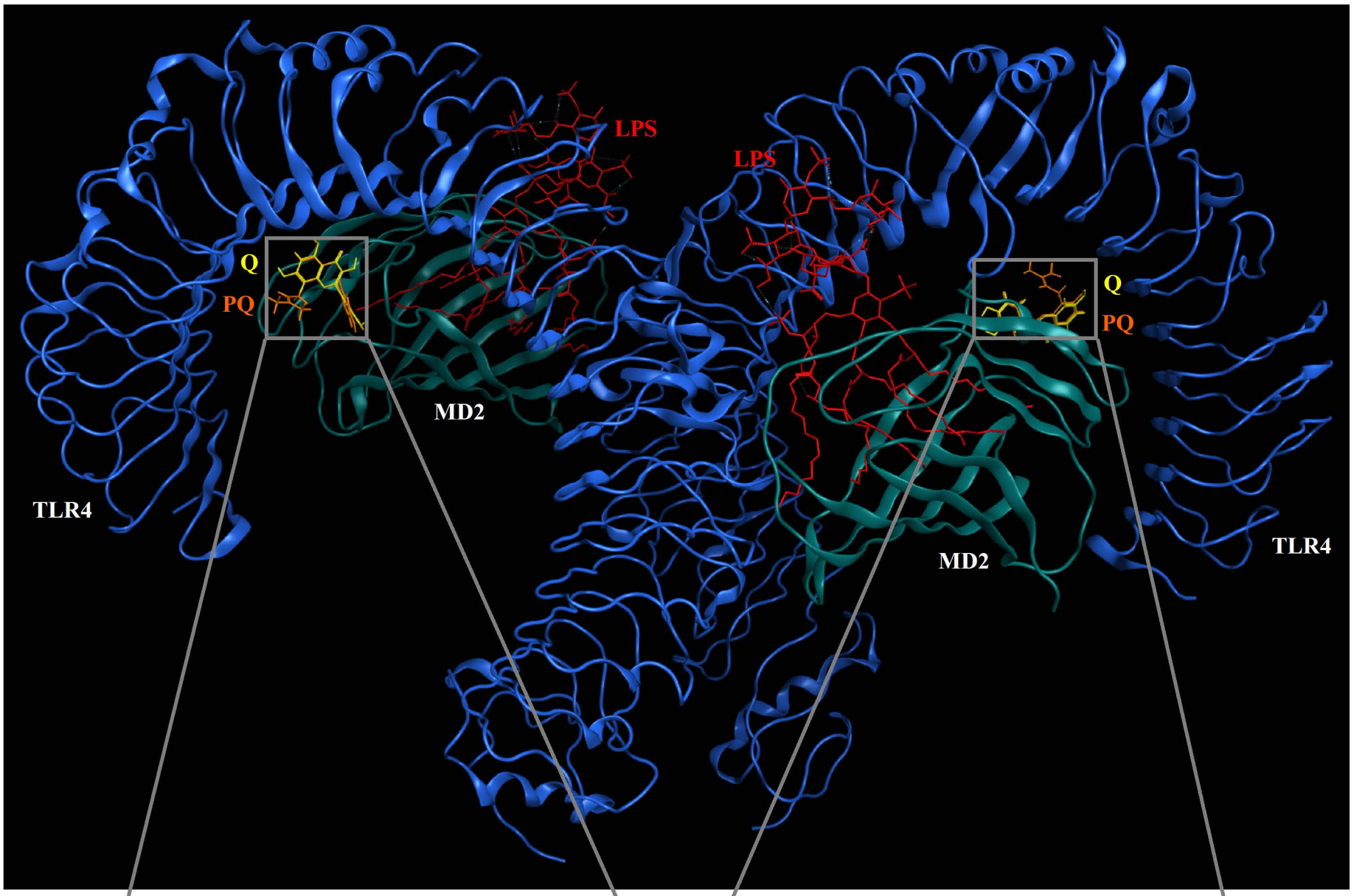

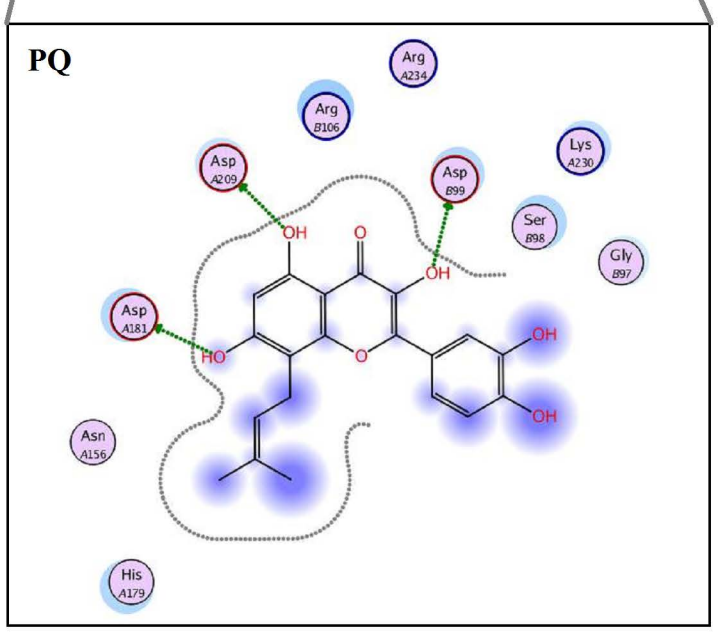

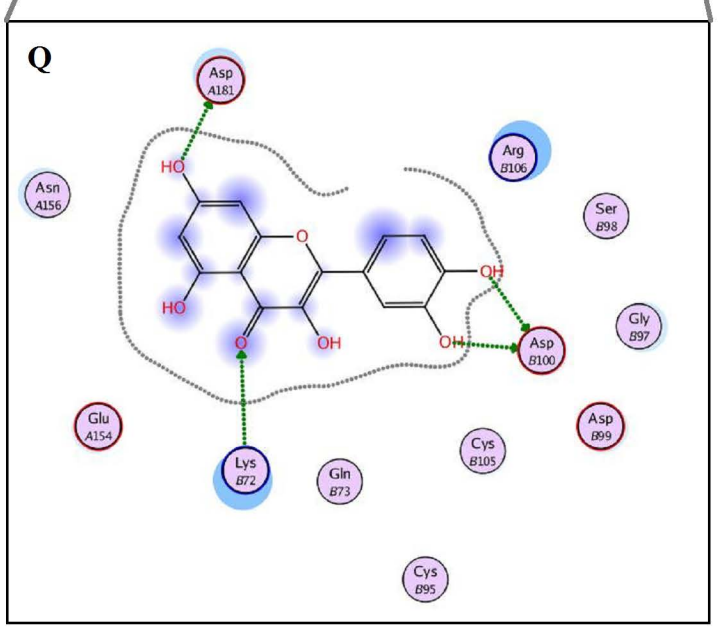

B

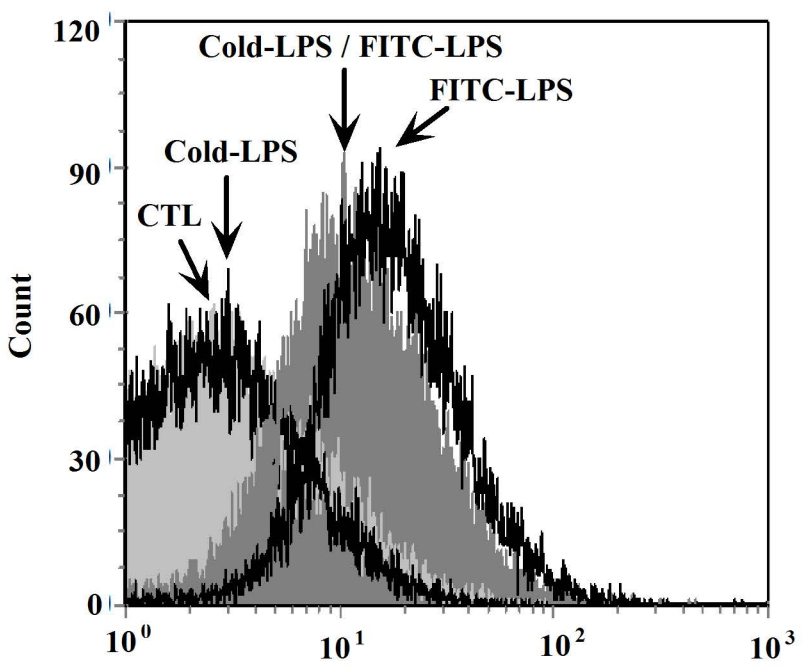

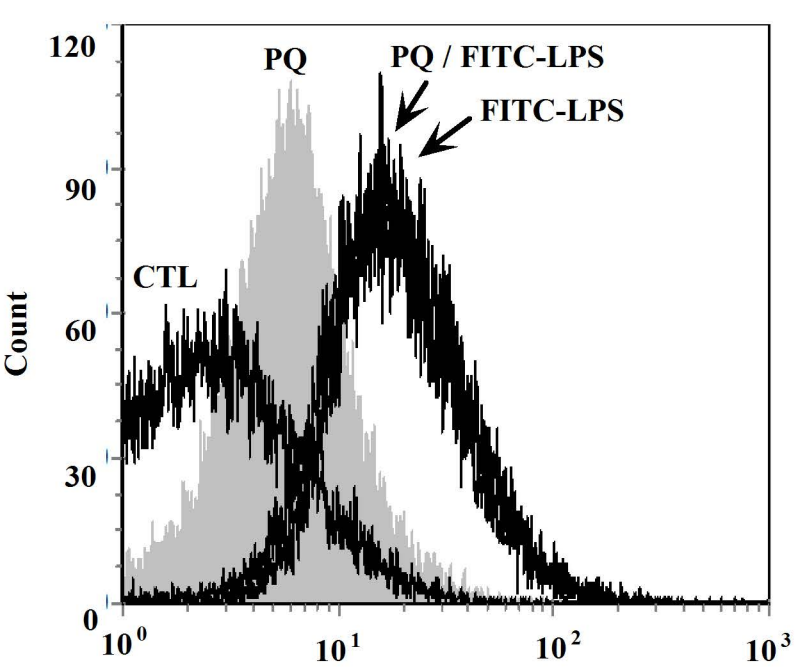

Fig.5 Hisanaga et al.

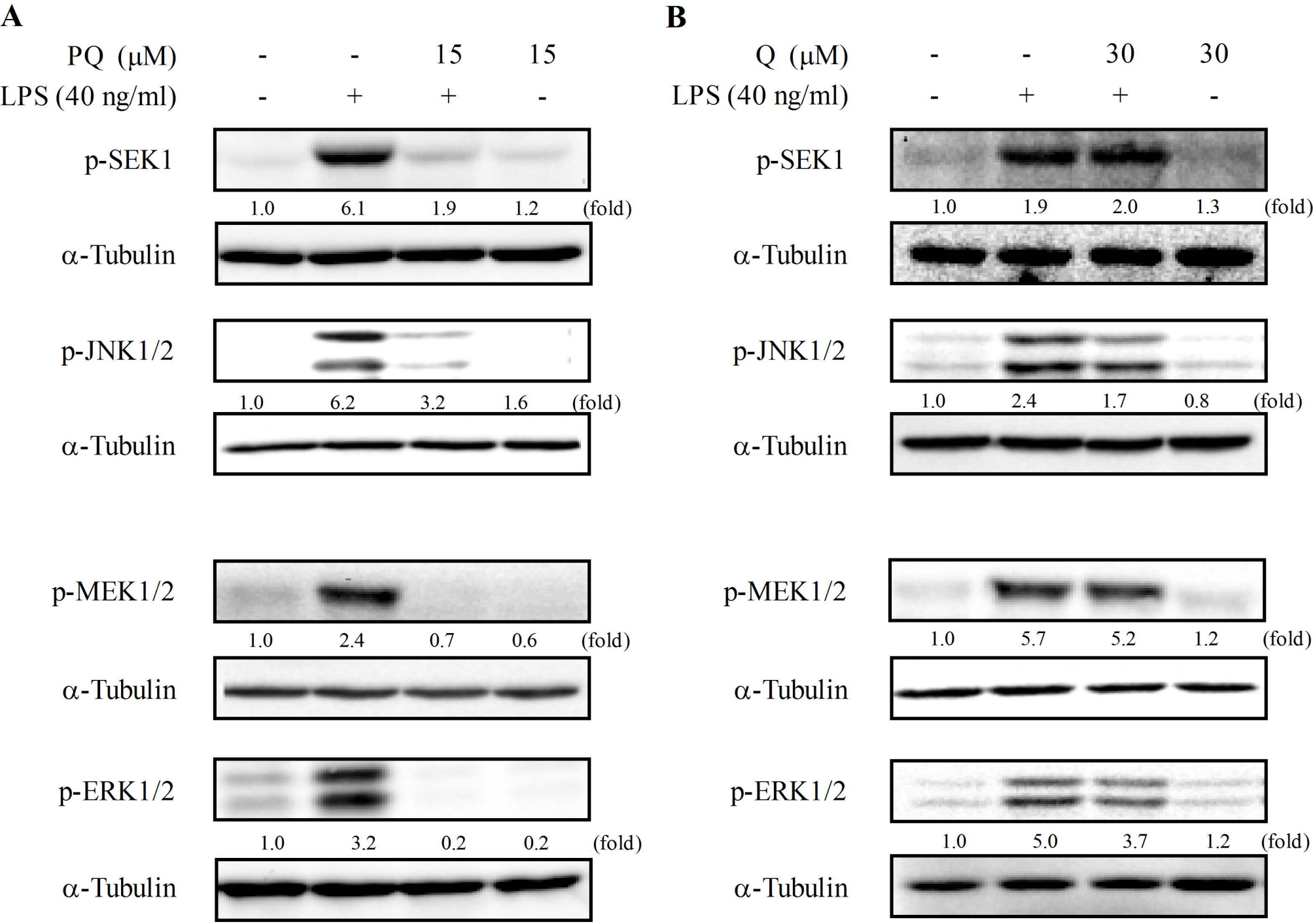

Fig. 6 Hisanaga et al.

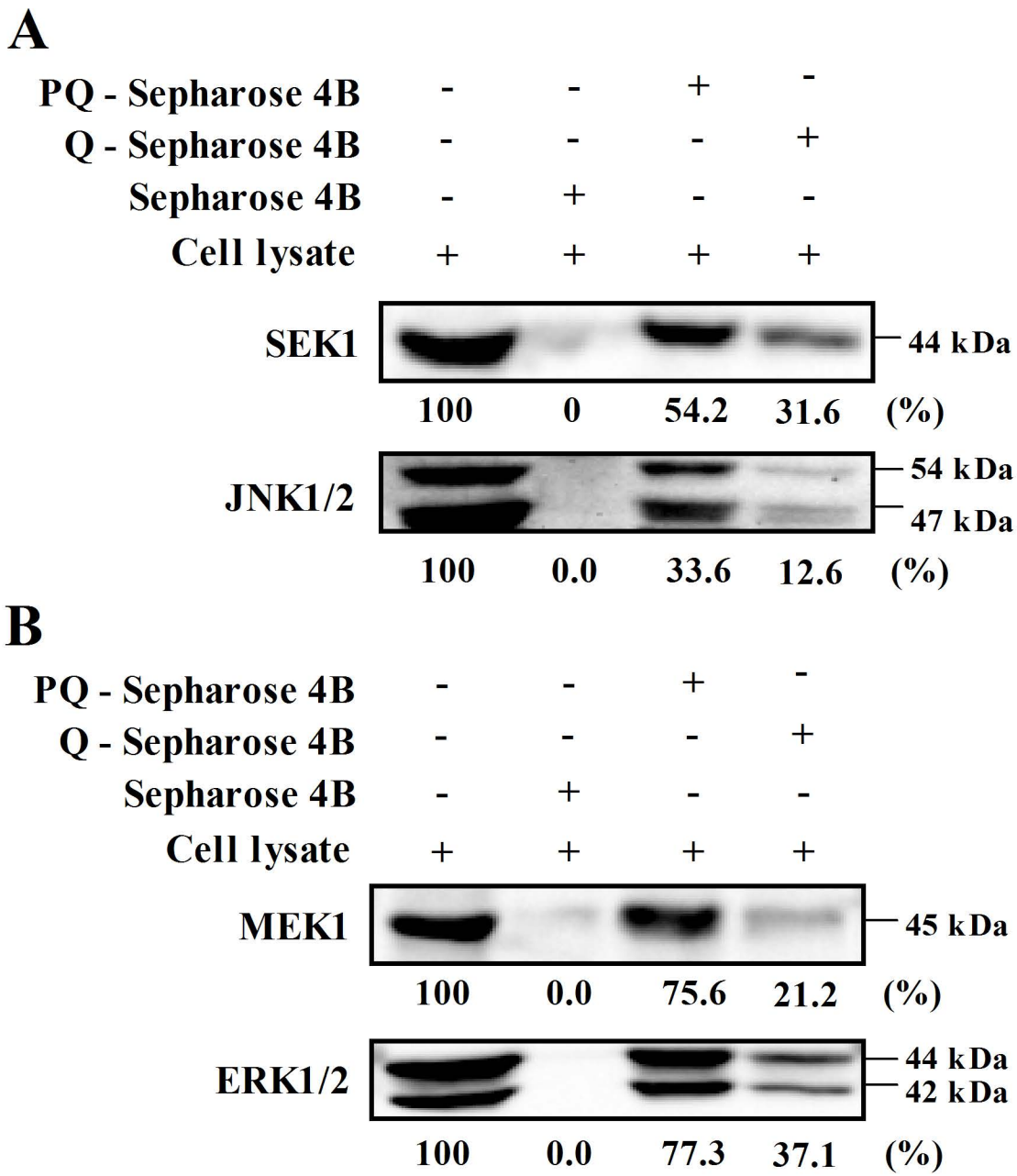

Fig.7 Hisanaga et al.

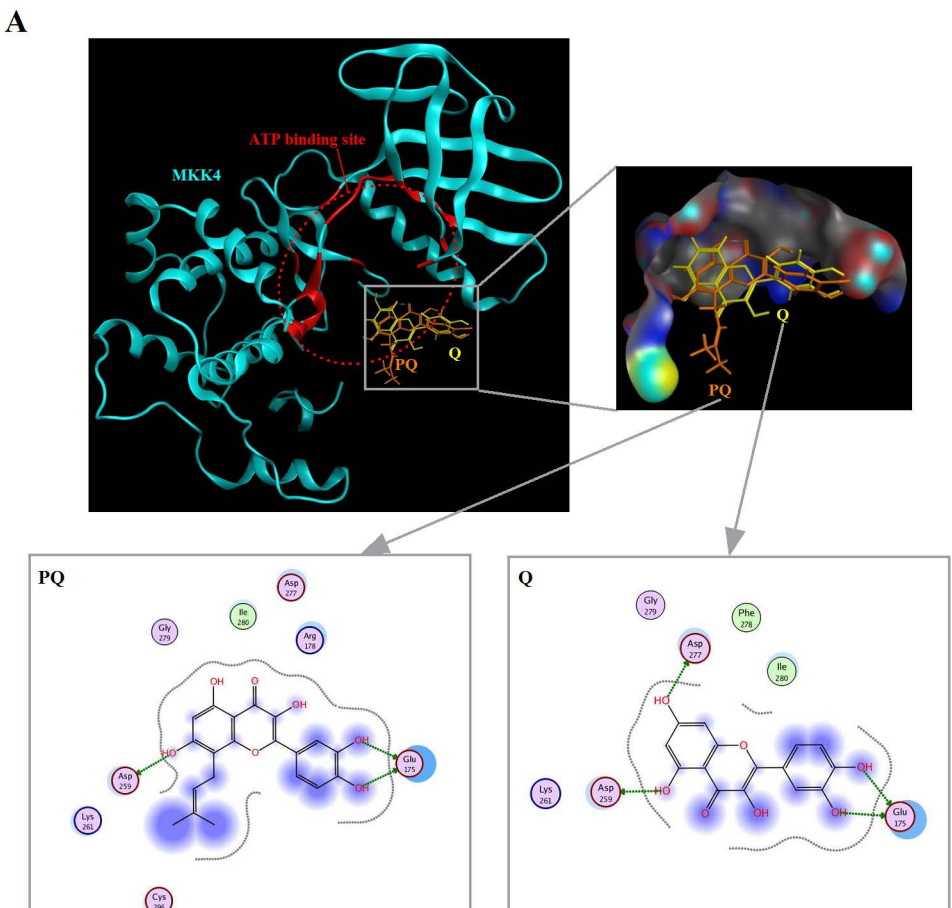

Fig.8 (A) Hisanaga et al.

B

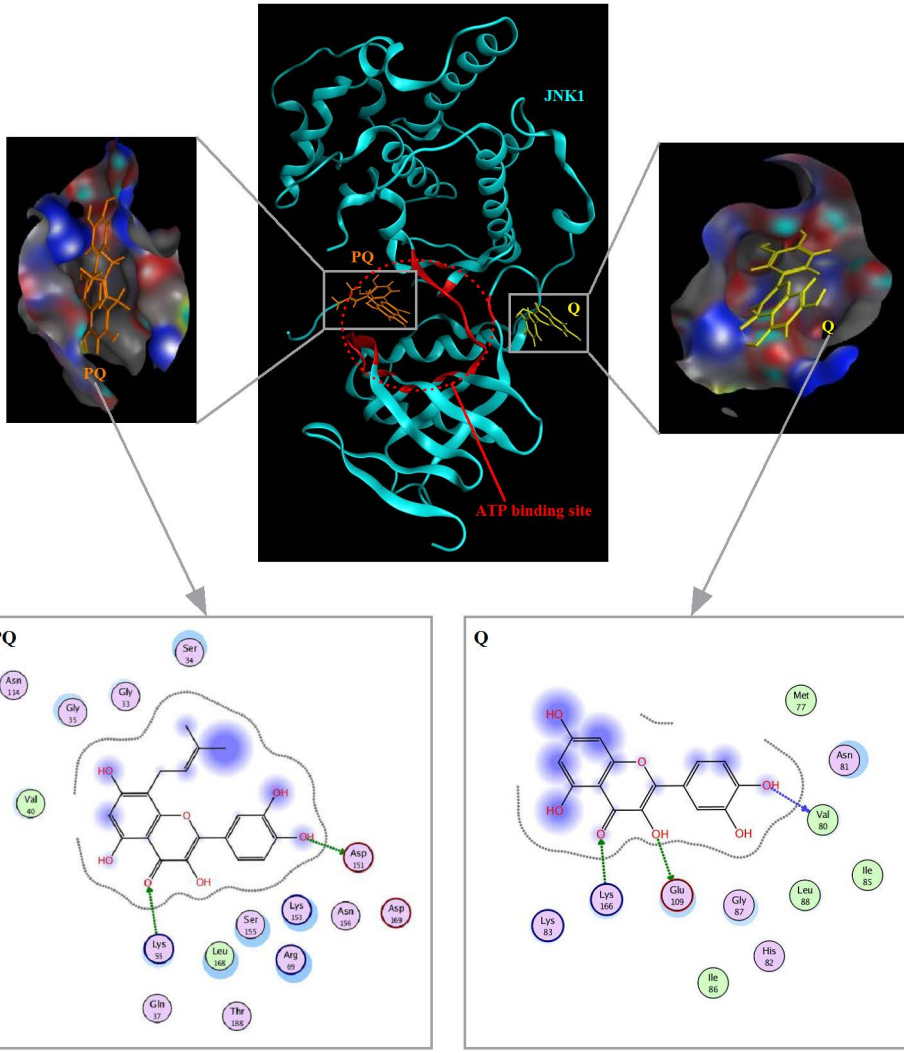

Fig.8 (B) Hisanaga et al.

C

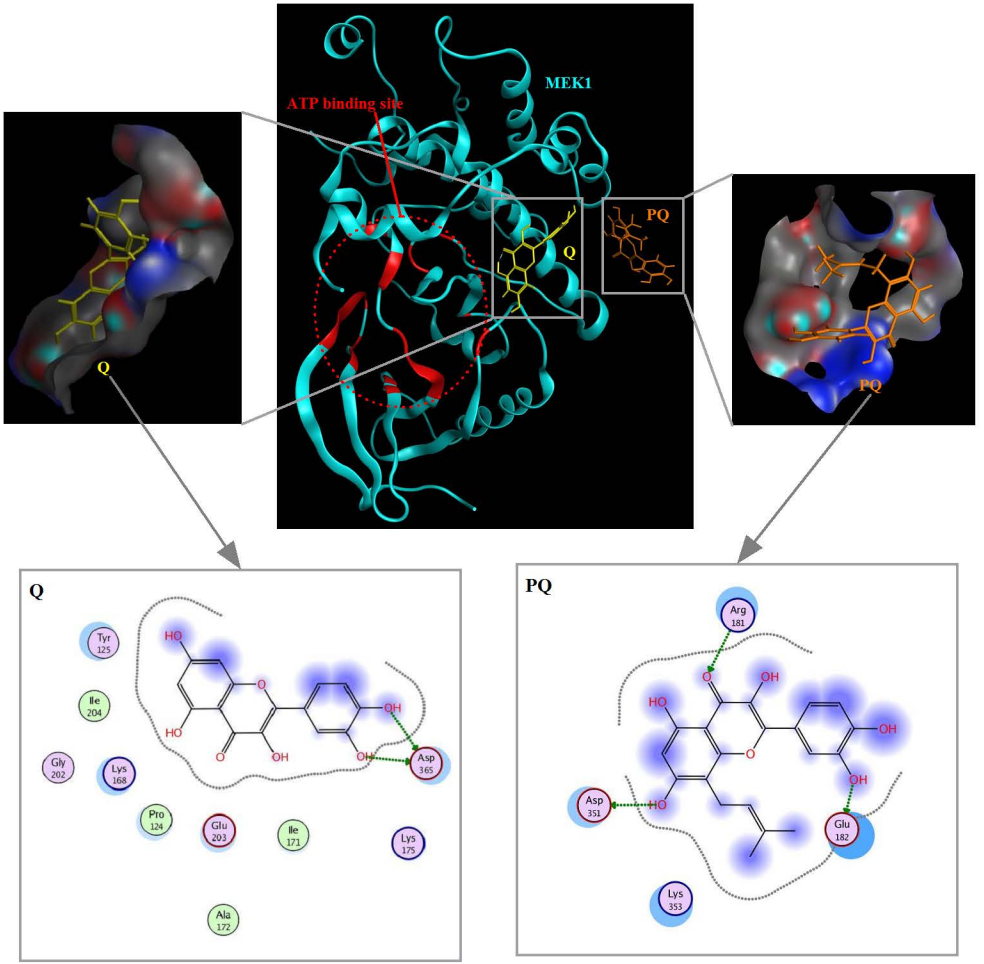

Fig.8 (C) Hisanaga et al.

D

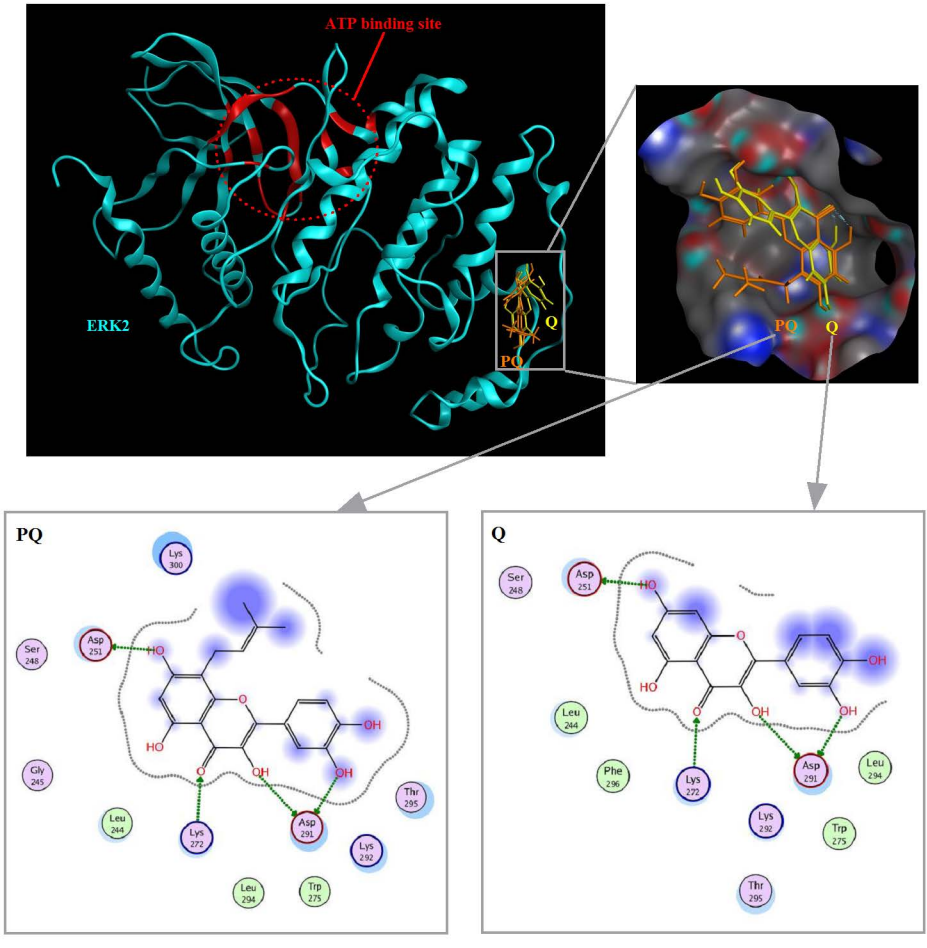

Fig.8 (D) Hisanaga et al.